

Supporting Information

High Efficient Solar Seawater Desalination with Environmentally Friendly Hierarchical Porous Carbons Derived from Halogen-containing Polymers

Fenghua Liu,^a Lijian Wang,^a Robert Bradley,^{b,c} Binyuan Zhao*^a, Weiping Wu*^d

^{a.} State Key Laboratory of Metal Matrix Composites, School of Materials Science and Engineering, Shanghai Jiao Tong University, Shanghai, 200240, China

^{b.} Department of Materials, University of Oxford, 16 Parks Road, Oxford, OX1 3PH, United Kingdom

^{c.} MatSurf Ltd, The Old Stables Marion Lodge, Little Salkeld, Penrith, Cumbria, CA10 1NW, United Kingdom

^{d.} Department of Electrical and Electronic Engineering, School of Mathematics, Computer Science and Engineering, City, University of London, Northampton Square, London, EC1V 0HB, United Kingdom

Content:

1. The dehalogenation of PVC
2. The pore structures of HPC
3. The X-ray Photoelectron Spectrum (XPS)
4. The Raman spectra
5. The typical TG results of the HPC samples
6. The solar reflectance spectrum of the flexible HPC samples
7. Energy Conversion Efficiency

1. The dehalogenation of PVC

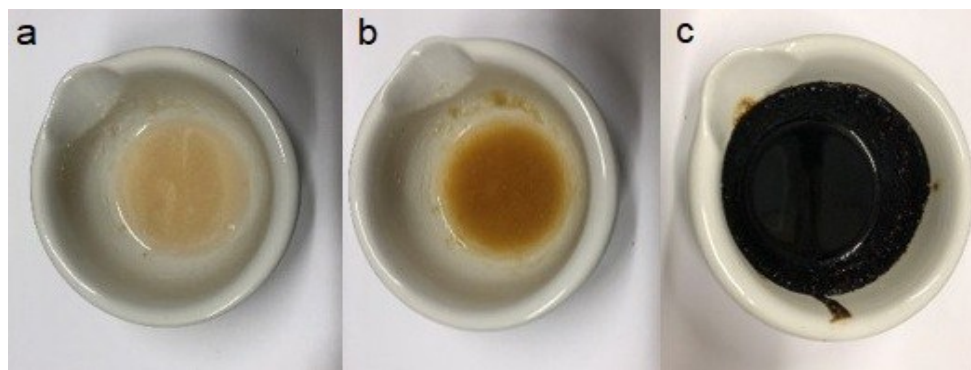


Fig. S1 Color changes of the room temperature dehalogenation process of Polyvinyl Chloride (PVC) by grinding for, (a) 0 min, (b) 3mins, (c) 10 mins. Dimethylformamide (DMF) was used as the solvent and the potassium hydroxide (KOH) is the dechlorination agent.

2. The pore structures of HPC

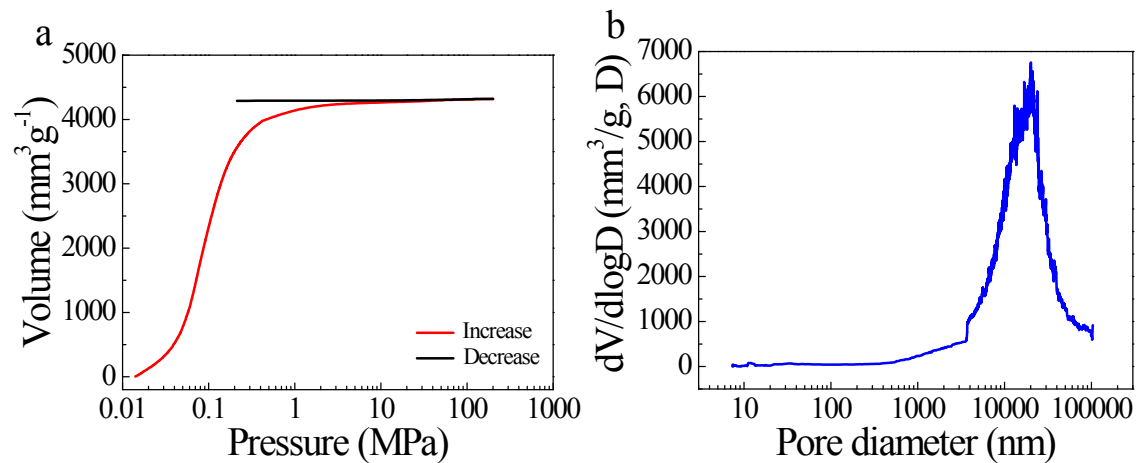


Fig. S2 The mercury intrusion porosimetry results of the HPC. (a) the pore volume with the pressure of mercury intrusion. (b) The typical pore diameter distribution.

3. The X-ray Photoelectron Spectrum (XPS)

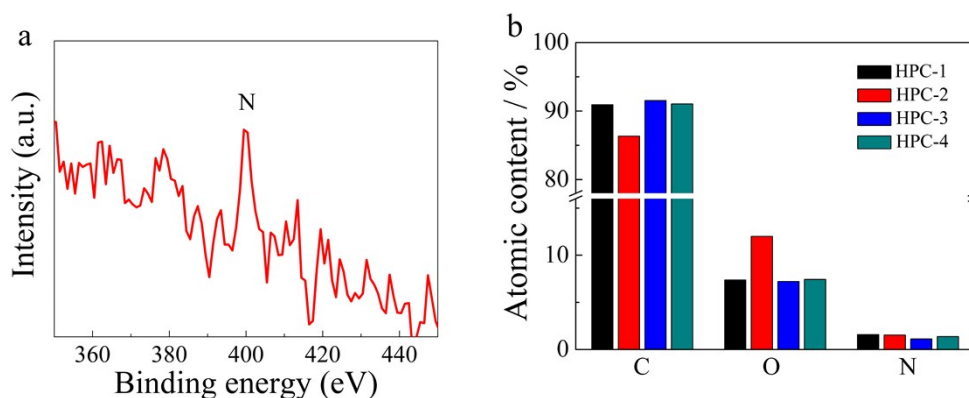


Fig. S3 a) The N1s peak by the X-ray Photoelectron Spectrum (XPS) of HPC-4, confirming the successful doping of nitrogen in the carbon material. b) The carbon (C), oxygen (O) and nitrogen (N) elemental concentrations in the samples.

4. The Raman spectra

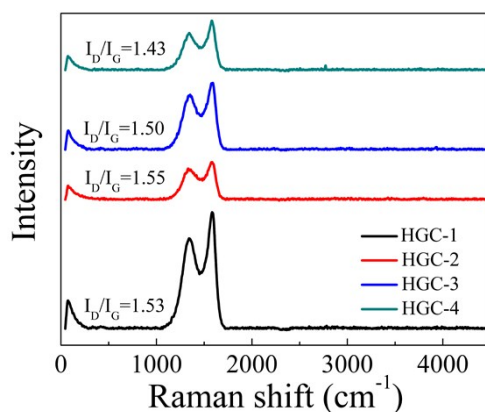


Fig. S4 The Raman spectra of HPC. The typical D-band ($\approx 1350\text{ cm}^{-1}$) induced by disorder is stronger than the G-band ($\approx 1575\text{ cm}^{-1}$) induced by in-plane vibrational, suggests a high density of defects. The graphitization degree depending on the amount of defects and disorder structures can be evaluated through the I_D/I_G ratio.^{1, 2} As the lower the I_D/I_G ratio, the higher the graphitization degree is. Raman spectra further reveal the structural evolution. The I_D/I_G ratio decreases with the time increase of mechanochemical grinding, suggesting that the number of defects and disorder structures decrease. The D

to G band intensity ratio (I_D/I_G) in HPC-4 is much lower than in the HPC-1 which revealed that graphitization degree increased.

5. The typical TG results of the HPC samples

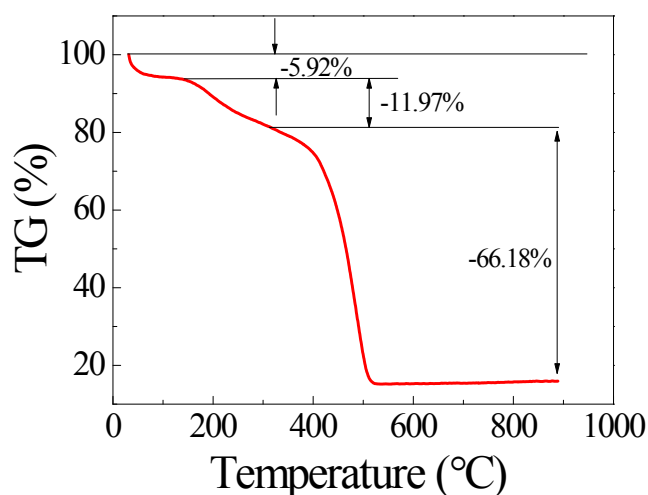


Fig. S5 The typical TG results of an HPC sample.

6. The solar reflectance spectrum of the flexible HPC samples

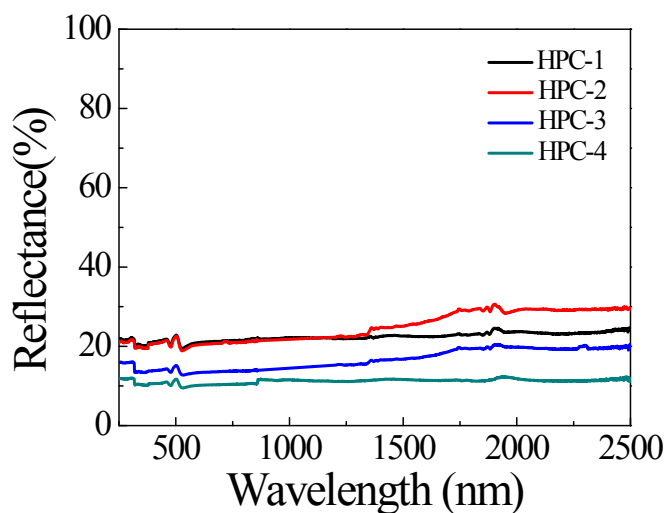


Fig. S6 The solar reflectance spectrum of the flexible HPC samples coated on papers collected from 250 nm to 2500 nm by the UV-Vis-NIR.

7. Energy Conversion Efficiency

The energy conversion efficiency (η_{th}) is a key figure that can be used to visually and efficiently evaluate the efficiency of the solar-to-vapor efficiency. It is defined as³,

$$\eta_{th} = \frac{\dot{m} h_{LV}}{C_{opt} q_i} \quad (1)$$

where \dot{m} is the mass loss rate of water per unit area which can be calculated from the mass loss curves at the steady state, h_{LV} is the evaporation enthalpy (sensible heat and liquid-vapour phase change), C_{opt} is the optical concentration, and q_i is the nominal direct solar irradiation of 1 kW m^{-2} . In our work, only the phase-change enthalpy is considered. And when calculating the evaporation rate, the natural evaporation rate in dark environment $0.224 \text{ kg m}^{-2} \text{ h}^{-1}$ will be subtracted (Figure S7).

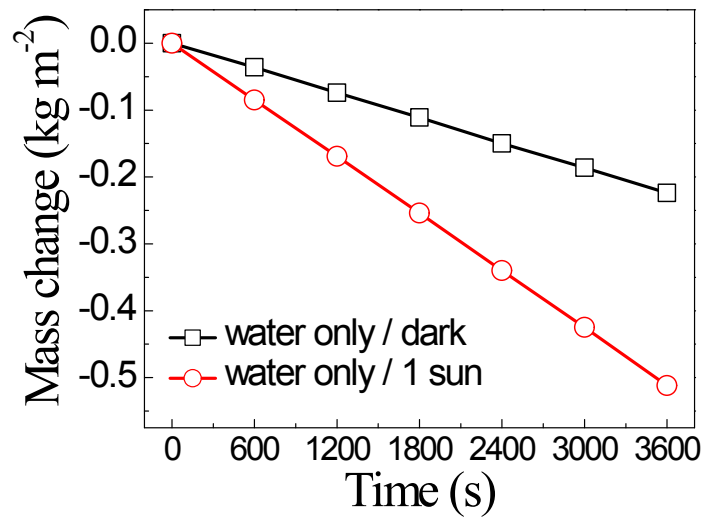


Fig. S7 The evaporation rates vs. time curves of water in the dark environment and under 1 sun irradiation (1 kW m^{-2}).

References

- 1 L. G. Cancado, A. Jorio, E. H. Ferreira, F. Stavale, C. A. Achete, R. B. Capaz, M. V. Moutinho, A. Lombardo, T. S. Kulmala and A. C. Ferrari, Quantifying defects in graphene via Raman spectroscopy at different excitation energies, *Nano Lett.*, 2011, **11**, 3190-3196.
- 2 A. C. Forse, C. Merlet, P. K. Allan, E. K. Humphreys, J. M. Griffin, M. Aslan, M. Zeiger, V. Presser, Y. Gogotsi and C. P. Grey, New Insights into the Structure of Nanoporous Carbons from NMR, Raman, and Pair Distribution Function Analysis, *Chem. Mater.*, 2015, **27**, 6848-6857.
- 3 P. Zhang, J. Li, L. Lv, Y. Zhao and L. Qu, Vertically Aligned Graphene Sheets Membrane for Highly Efficient Solar Thermal Generation of Clean Water, *ACS Nano*, 2017, **11**, 5087-5093.